

# Dissecting Quantization Error: A Concentration-Alignment Perspective

Marco Federici<sup>1</sup> Boris van Breugel<sup>1</sup> Paul Whatmough<sup>1</sup> Markus Nagel<sup>1</sup>

## Abstract

Quantization can drastically increase the efficiency of large language and vision models, but typically incurs an accuracy drop. Recently, function-preserving transforms (e.g. rotations, Hadamard transform, channel-wise scaling) have been successfully applied to reduce post-training quantization error, yet a principled explanation remains elusive. We analyze linear-layer quantization via the signal-to-quantization-noise ratio (SQNR), showing that for uniform integer quantization at a fixed bit width, SQNR decomposes into (i) the concentration of weights and activations (capturing spread and outliers), and (ii) the alignment of their dominant variation directions. This reveals an actionable insight: beyond concentration — the focus of most prior transforms (e.g. rotations or Hadamard) — improving alignment between weight and activation can further reduce quantization error. Motivated by this, we introduce block Concentration–Alignment Transforms (CAT), a lightweight linear transformation that uses a covariance estimate from a small calibration set to jointly improve concentration and alignment, approximately maximizing SQNR. Experiments across several LLMs show that CAT consistently matches or outperforms prior transform-based quantization methods at 4-bit precision, confirming the insights gained in our framework.

## 1. Introduction

Model quantization is the most fundamental strategy to reduce computation and memory requirements for large models such as LLMs. However, drastic reduction in performance is often observed when quantizing model weights and activations at lower bit-widths. Recently, the introduction of invertible linear transformations (Xiao et al., 2024; Ashkboos et al., 2024; van Breugel et al., 2025), which

<sup>1</sup>Qualcomm AI Research. Qualcomm AI Research is an initiative of Qualcomm Technologies, Inc. Correspondence to: <{mfederic,bvanbreu,pwhatmou,markusn}@qualcomm.com>.

Preprint. March 5, 2026.

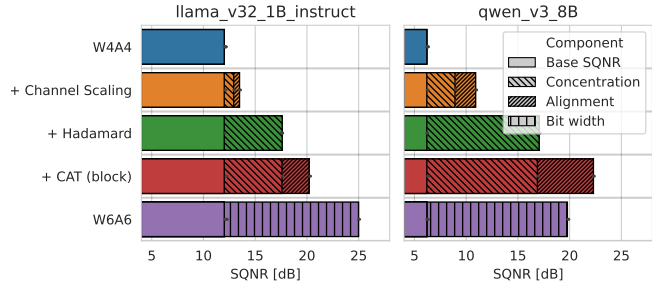


Figure 1. The signal-to-quantization-noise (SQNR) of a quantized linear layer can be factorized into a bit width term, concentration, and alignment. Orthogonal transforms (e.g. Hadamard, rotation) can improve the concentration (reduce outliers), but not the alignment. Concentration-Alignment Transform (CAT) is designed to improve alignment too, which yields a W4A4 SQNR that often rivals W6A6 quantization.

are partially fused into the model weights, have enabled more aggressive compression at the small cost of additional operations during inference. Popular linear transforms include rotations (Ashkboos et al., 2024; Liu et al., 2024; Tseng et al., 2024), element-wise scaling (Xiao et al., 2024; Shao et al., 2024), kronecker-factorized matrices (Sun et al., 2025), or combinations thereof (Hu et al., 2025). Each transform aids in recovering performance on quantized models; however, the literature remains scattered and no consensus on how to achieve an optimal transform has been reached. The contributions of this paper are as follows:

- We introduce a novel framework to interpret the specific origins of quantization error, disentangling a concentration and an alignment term (Section 2).
- We demonstrate the effectiveness of our framework on LLM linear layers, analyzing how existing transforms improve quantization in terms of concentration and alignment. We further demonstrate that popular, rotation-based approaches (incl. Hadamard) completely neglect the alignment component of quantization error (Section 3).
- We derive Concentration-Alignment Transform (CAT) as a theoretically motivated training-free transform that optimizes both components, but is too costly for practice. We show that approximating the CAT-optimal

transform with a block-diagonal matrix (comparable in cost to existing solutions) still provides improvements in alignment and concentration, resulting in state-of-the-art accuracy on common LLM benchmarks (Sections 4 and 6).

## 2. Concentration-Alignment Framework

For a quantized linear layer  $\widetilde{\mathbf{W}}\widetilde{\mathbf{x}}$  with quantized weights  $\widetilde{\mathbf{W}} \stackrel{\text{def}}{=} Q_W(\mathbf{W})$  and quantized activations  $\widetilde{\mathbf{x}} \stackrel{\text{def}}{=} Q_x(\mathbf{x})$ , the Signal to Quantized Noise Ratio (SQNR) on the layer output is defined as:

$$\text{SQNR}(\widetilde{\mathbf{W}}\widetilde{\mathbf{x}}) \stackrel{\text{def}}{=} \frac{\mathbb{E} \left[ \|\mathbf{W}\mathbf{x}\|_2^2 \right]}{\mathbb{E} \left[ \|\mathbf{W}\mathbf{x} - \widetilde{\mathbf{W}}\widetilde{\mathbf{x}}\|_2^2 \right]}. \quad (1)$$

SQNR is a standard metric to measure the effect of the quantization noise since it measures the ratio of the magnitude of the signal (numerator) compared to the the quantization noise (denominator).

Using standard error de-correlation assumptions (Widrow et al., 1996), the SQNR of a quantized linear layer can be approximated as a function of the SQNR obtained by quantizing only activation and weights, respectively.

**Lemma 2.1.** *The SQNR of a quantized linear layer can be approximated with the harmonic sum (parallel) of the SQNR measured by quantizing activations and weights separately:*

$$\text{SQNR}(\widetilde{\mathbf{W}}\widetilde{\mathbf{x}}) \approx \text{SQNR}(\mathbf{W}\widetilde{\mathbf{x}}) \parallel \text{SQNR}(\widetilde{\mathbf{W}}\mathbf{x}),$$

in which  $\parallel$  refers to the *parallel* operator:  $a \parallel b = (1/a + 1/b)^{-1}$ .

Based on the independence of the components of the quantization error (Gersho, 1977), we show the following.

**Lemma 2.2.** *Whenever the clipping error is small, the SQNR for uniform integer-quantized activations can be approximated as the product of three main components:*

$$\text{SQNR}(\mathbf{W}\widetilde{\mathbf{x}}) \approx 12 \underbrace{(2^{b_x} - 1)^2}_{N(b_x)} \underbrace{\frac{\mathbb{E} \left[ \|\mathbf{x}\|_2^2 \right]}{\mathbb{E} \left[ r(\mathbf{x})^2 \right]}}_{C(\mathbf{x})} \underbrace{\frac{\mathbb{E} \left[ \|\mathbf{W}\mathbf{x}\|_2^2 \right]}{\|\mathbf{W}\|_F^2 \mathbb{E} \left[ \|\mathbf{x}\|_2^2 \right]}}_{A(\mathbf{x}, \mathbf{W})},$$

in which  $b_x$  refers to the number of bits used to quantize the activations,  $\|\mathbf{W}\|_F^2$  indicates the squared Frobenius norm of the weights, and  $r(\mathbf{x})$  expresses the quantization range of the activations, which may be *static* (constant in  $\mathbf{x}$ ) or *dynamic* (dependent on  $\mathbf{x}$ ). This is usually defined as  $\max_i \mathbf{x}_i - \min_i \mathbf{x}_i$  for *asymmetric* quantization and  $2 \max_i |\mathbf{x}_i|$  for *symmetric* quantization.

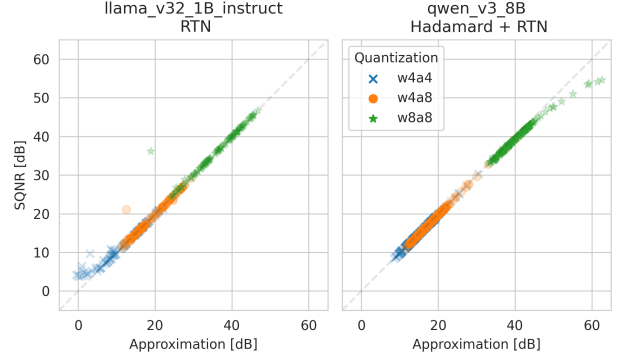


Figure 2. Empirical verification of the approximation reported in Theorem 2.4 for linear layers of LLama-v32-1B (left) and Qwen-v3-8B with Hadamard rotations applied before every linear layer (right) at W4A4, W4A8 and W8A8 quantization. Each dot represents one linear layer in the architecture. The approximation is close to the true SQNR for almost all layers. *In L3.2 1B-it, the exception is layer.1.mlp.down.proj, which is easier to quantize than the approximation suggests, due to the massive outlier of the [BOS] token (Sun et al., 2024) dominating the SQNR computation. For large SQNR, floating point issues limit the true SQNR (Qwen v3, top right).*

A similar derivation can be used to approximate the SQNR for weight quantization.

**Lemma 2.3.** *For negligible clipping error, the SQNR for uniform integer-quantized weights can be written as:*

$$\text{SQNR}(\widetilde{\mathbf{W}}\mathbf{x}) \approx 12 \underbrace{(2^{b_w} - 1)^2}_{N(b_w)} \underbrace{\frac{\sum_i \|\mathbf{w}_i\|_2^2}{\sum_i r(\mathbf{w}_i)^2}}_{C(\mathbf{W})} \underbrace{\frac{\mathbb{E} \left[ \|\mathbf{W}\mathbf{x}\|_2^2 \right]}{\|\mathbf{W}\|_F^2 \mathbb{E} \left[ \|\mathbf{x}\|_2^2 \right]}}_{A(\mathbf{x}, \mathbf{W})},$$

with  $b_w$  as the number of bits used to quantize each element in a row of  $\mathbf{W}$ .

Using the result from Lemma 2.1, 2.2, and 2.3, we formulate an overall approximation for the SQNR of quantized linear layers.

**Theorem 2.4.** *Whenever the clipping error is negligible, the SQNR for a quantized linear layer can be approximated as:*

$$\text{SQNR}(\widetilde{\mathbf{W}}\widetilde{\mathbf{x}}) \approx 12 (N(b_x)^2 C(\mathbf{x}) \parallel N(b_w)^2 C(\mathbf{W})) A(\mathbf{x}, \mathbf{W}).$$

Figure 2 empirically verifies the validity of the proposed approximation, comparing directly the measured SQNR and the value reported in Theorem 2.4 for linear layers of LLMs quantized at different bit widths with (right) and without (left) linear transformations. We observe that the reported approximation is accurate for the vast majority of layers between 5 and 50 decibels (dB), making it useful in practice.

Note that  $N(b_x)$  and  $N(b_w)$  indicate the number of quantization intervals, which depend solely on the chosen bit

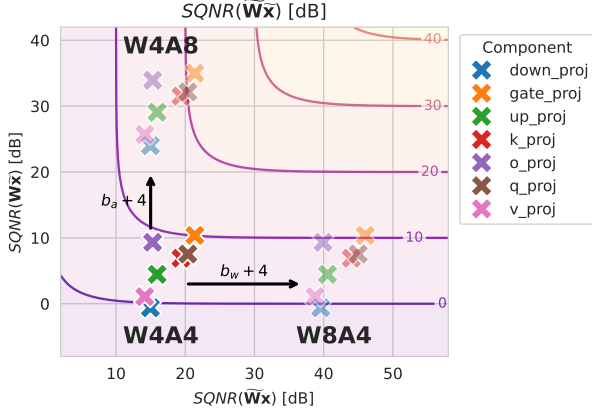


Figure 3. Comparison of activation quantization SQNR (y-axis), weight quantization SQNR (x-axis) and joint SQNR (iso-lines) for the linear layers of a Llama v3 8B architecture quantized at several bit widths. Starting from a 4 bit quantization of the linear layer (bottom left), increasing the weight bit width by 4 bits will result in a horizontal shift of around 24 dB, while increasing number of bits used for the activations results in a corresponding vertical shift. Since activation SQNR is worse than weight SQNR ( $r(\mathbf{x}, \mathbf{W}) < 1$ ), this latter scenario results in much higher overall SQNR.

width. We will refer to  $C(\mathbf{x})$  and  $C(\mathbf{W})$  as measure of activation and weight *Concentration*, respectively, while we denote  $A(\mathbf{x}, \mathbf{W})$  as a measure of second-order activation and weight *Alignment*. In the following, we explore the role of each component in Theorem 2.4 in more depth.

### 2.1. Interactions of Bit width, Concentration and Alignment

**Bit width** The term  $N(b_x)$  represents the number of distinct quantization intervals for  $\mathbf{x}$  (similarly,  $N(b_w)$  for  $\mathbf{W}$ ). This term only depends on the number of bits used to quantize  $\mathbf{x}$  (and  $\mathbf{W}$ ). Higher bit width can be further used to compensate for poor weight/activation concentration. As illustrated in Figure 3, increasing the bit width of weights or activations, effectively increases overall SQNR. However, the magnitude of the increase depends on the ratio between  $\text{SQNR}(\mathbf{W}\tilde{\mathbf{x}})$  and  $\text{SQNR}(\tilde{\mathbf{W}}\mathbf{x})$ , which corresponds to scenarios in which only activations or weights are quantized, respectively:

$$r(\mathbf{x}, \mathbf{W}) \stackrel{\text{def}}{=} \frac{\text{SQNR}(\mathbf{W}\tilde{\mathbf{x}})}{\text{SQNR}(\tilde{\mathbf{W}}\mathbf{x})} = \frac{b_x}{b_w} \frac{C(\mathbf{x})}{C(\mathbf{W})}. \quad (2)$$

Whenever the activation SQNR is smaller than the weight SQNR ( $r(\mathbf{x}, \mathbf{W}) < 1$ ), increasing the weight bit width  $b_w$  will have less effect than increasing the activation bit width  $b_x$ , and vice versa for  $r(\mathbf{x}, \mathbf{W}) > 1$ . In other words, the overall SQNR for the linear layer is mostly determined by its worst component.

Whenever activations and weights are quantized at the same bit width  $b_w = b_x = b$ , the equation in Theorem 2.4 can be simplified to:

$$\text{SQNR}(\tilde{\mathbf{W}}\tilde{\mathbf{x}}) \approx 12N(b)^2 (C(\mathbf{x}) \| C(\mathbf{W}))A(\mathbf{x}, \mathbf{W}). \quad (3)$$

In this scenario, the effect of increasing the (joint) bit width  $b$  can be disentangled from the other terms, and each extra bit increases joint SQNR approximately by a factor 4 (about 6 dB). However, increasing bit width incurs extra memory and compute costs. For this reason, in this paper, we will mostly focus on improving concentration and alignment for a fixed bit width quantization.

**Concentration**  $C(\mathbf{W})$  and  $C(\mathbf{x})$  can be seen as measures of *Concentration*, which defines the spread of the rows  $w$  of the weights  $\mathbf{W}$  and activation distributions  $\mathbf{x} \sim p(\mathbf{x})$ , respectively. Concentration is strongly related to the measure of kurtosis (Akhondzadeh et al., 2025), which considers the ratio between norm 4 and norm 2. Similarly, concentration captures the ratio between the squared norm 2 and squared norm infinity (range). Like kurtosis, concentration is scale-invariant and depends only on the weight and activation distributions.

For heavy-tailed distributions, in the presence of outliers, the concentration is low, while for distributions that collapse into a single value the concentration grows to infinity. For asymmetric quantization the lowest concentration is  $1/2$  ( $-3$  dB), while for symmetric quantization, the smallest value is  $1/4$  ( $-6$  dB), corresponding to a single non-zero value. Switching from a symmetric to an asymmetric quantization scheme can drastically reduce the quantization scale whenever the data is shifted or strongly asymmetric (e.g. activations after a *ReLU* function), drastically improving concentration. However, asymmetric quantization yields only negligible improvements for symmetric, zero-centered distributions, which are common in modern LLMs.

Increasing activation or weight concentration has an analogous effect to increasing the corresponding bit width: whenever  $r(\mathbf{x}, \mathbf{W}) < 1$ , as in the examples reported in Figure 3 and Figure 4, improving activation concentration will have significantly more effect than improving the concentration of the corresponding weight.

**Alignment**  $A(\mathbf{x}, \mathbf{W})$ , on the other hand, can be interpreted as an *Alignment* term, which measures the similarity between the directions of variation of the weights and activations. Similar to concentration, alignment is also scale-invariant. Furthermore, alignment between activation and weights is not affected by rotations; for any orthogonal

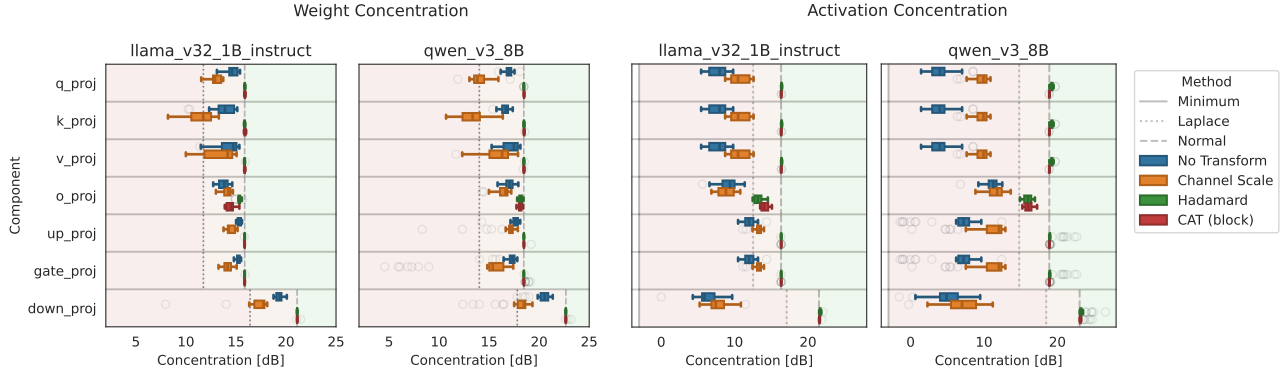


Figure 4. Distribution of concentration of weight (left) and activation (right) quantization, for different layers and under different transforms. Activations are more heavy-tailed (worse than Laplace, red region) than weights, without transforms. Channel scaling (such as SmoothQuant) moves the activation outliers into the weights—this improves activation concentration, but worsens weight concentration significantly. Hadamard and CAT mix channels, which effectively makes them close to Gaussian for all layers.

matrix  $\mathbf{R}$ :

$$A(\mathbf{R}\mathbf{x}, \mathbf{W}\mathbf{R}^T) = \frac{\mathbb{E}[\|\mathbf{W}\mathbf{R}^T\mathbf{R}\mathbf{x}\|_2^2]}{\|\mathbf{W}\mathbf{R}^T\|_F^2 \mathbb{E}[\|\mathbf{R}\mathbf{x}\|_2^2]} = A(\mathbf{x}, \mathbf{W}). \quad (4)$$

In other words, rotating the activations of a linear layer by  $\mathbf{R}$  and the corresponding weight by  $\mathbf{R}^T$  will have no effect on their alignment.

It is important to realize that the alignment term  $A(\mathbf{x}, \mathbf{W})$  is a multiplier in each of the SQNR expressions. Therefore, improving alignment between activations and weights yields better SQNR for both weight and activation quantization, independent of the respective bit widths or concentration. Improving alignment by a factor  $k$  has the same effect of increasing both activation and weight bit widths by approximately a factor  $\log_2 \sqrt{k}$ . Across various LLMs we consistently observe that some layers (such as *down\_proj*, *o\_proj* and *v\_proj*) display significantly worse alignment than the other layers (Figure 5). This raises the question: what is the best possible alignment? And how can we achieve it? In the next section, we answer this question by analyzing the impact of common linear transformations on weight and activation concentration and alignment.

### 3. Analysis of Linear Transformations

Given a linear layer, we consider an invertible linear transformation represented by matrix  $\mathbf{T}$ , which acts on activation and weights before quantizing:

$$\mathbf{W}\mathbf{x} = \mathbf{W}\mathbf{T}^{-1}\mathbf{T}\mathbf{x} \approx \underbrace{Q(\mathbf{W}\mathbf{T}^{-1})}_{\widetilde{\mathbf{W}}\mathbf{T}^{-1}} \underbrace{Q(\mathbf{T}\mathbf{x})}_{\widetilde{\mathbf{T}}\mathbf{x}}. \quad (5)$$

Clearly,  $\mathbf{T}$  can be optimized to improve SQNR. In particular, it is easy to show that there are transformations for which

the SQNR does not decrease:

$$\text{SQNR}(\widetilde{\mathbf{W}}\widetilde{\mathbf{x}}) \leq \max_{\mathbf{T}} \text{SQNR}(\widetilde{\mathbf{W}}\mathbf{T}^{-1}\widetilde{\mathbf{T}}\mathbf{x}). \quad (6)$$

Optimizing for  $\mathbf{T}$  directly can be challenging due to the discretization in the quantization function. Instead, using the expression in Theorem 2.4, we can interpret  $\mathbf{T}$  based on its effect on concentration and alignment.

In this section, we support our theoretical analysis with empirical observations collected by transforming linear layers of a *Llama v3.2 1B* and *Qwen v3* architectures. For each experiment, we apply transform  $\mathbf{T}$  before each linear layer and its inverse  $\mathbf{T}^{-1}$  on the weight of each linear layer. For layers that use the same input activations (such as *q\_proj* / *k\_proj* / *v\_proj* and *up\_proj* / *gate\_proj*) we use the same transformation, treating the layer as a single linear layer with multiple output heads. The results are visualized in Figures 4, 5 and 6.

Xiao et al. (2024) introduce channel-wise scaling  $\mathbf{T}_{\text{channel}} = \text{Diag}([s_1, \dots, s_d])$ , with  $s_i = (\max_{\mathbf{x}} x_i)^\alpha / (\max_{w_j} w_{ji})^{1-\alpha}$  to balance scale of activation and weight channels, effectively improves SQNR by re-distributing outliers between weights and activations. This operation has essentially two effects. First, the activation concentration is improved at the cost of lower weight concentration (Figure 4). As discussed in the previous section and visualized in Figure 6, this effect is overall beneficial since the overall SQNR is mostly determined by the worse concentration. Secondly, this channel-balancing operation has a slightly positive effect of activation and weight alignment for most layers in the architecture (Figure 5) although the overall impact of the improved alignment on SQNR is not very significant.

A common choice of transformation that reduces the effect of outliers is the family of Hadamard matrices  $\mathbf{H}$  (Ashk-

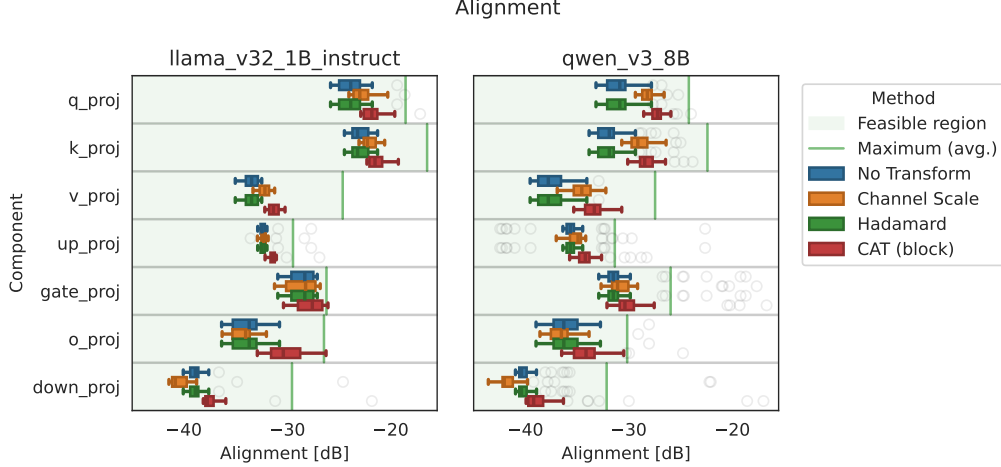


Figure 5. Distribution of alignment across layers under different transforms. The green shaded region indicates the achievable region, and underlines vast room for alignment improvements ( $> 10$  dB) on many layers. Note that rotation-based transforms cannot improve alignment, hence Hadamard transforms performs the same as no transforms. Channel scaling is similar to an alignment-optimal with block size 1. However, due to the sub-optimality scaling the channels using the ratio of the maximums does not necessarily improve on alignment on all layers. Block-diagonal matrices informed by CAT are good approximations of  $\hat{M}$ , and consistently improve alignment across all layers.

boos et al., 2024; Liu et al., 2024; Hu et al., 2025; Chee et al., 2024). Under the common assumption of channel independence, we can intuitively understand the effect of Hadamard rotations as the averaging of random variables, which causes the channel distribution to approach a Normal distribution by the central limit theorem. The concentration of Hadamard-transformed weights and activations approaches the concentration of a multivariate  $d$ -dimensional Normal distribution:  $\mathcal{N}(\mathbf{0}, \mathbf{I})$ . This is empirically visualized in Figure 4, where the Normal concentration is visualized with vertical dashed lines depending on the dimensionality of the layer.

The activation concentration for most activations in the model is worse than Laplace (red region), indicating the presence of heavy tails and severe outliers, while weight generally exhibit concentration in between the one of a Laplace and a Normal distribution (yellow region). In most layers, a Hadamard rotation suffices to significantly improve the concentration. This improvement is particularly evident for larger layers of bigger architectures, such as the *down\_proj* layer in the Qwen v3 8B model, in which a Hadamard rotation results in an improvement in activation concentration of more than 10 decibels. As show in Figure 6, compared to channel scaling, Hadamard transformations have a much more pronounced effect on the overall SQNR, drastically improving both activation and weight concentration.

However, any orthogonal linear transformation has no impact on activation and weight alignment. In fact, while optimizing concentration (or similar proxies) is a common practice in literature, alignment is often neglected. In par-

ticular, it is crucial to consider that alignment is **invariant to rotations**, hence approaches that rely solely on rotations  $\mathbf{R}$  yield no improvement on alignment, as demonstrated in Figure 5.

#### 4. Concentration-Alignment Transforms

In this section we design transforms that effectively optimizes both concentration and alignment.

**Optimizing alignment** In order to improve on alignment, we take a closer look to determine which transformations  $\hat{M}$  are optimal for  $A(\hat{M}\mathbf{x}, \mathbf{W}\hat{M})$ . Interestingly, the maximization admits an analytical solution, which is determined by the matrix geometric mean (Pusz & Woronowicz, 1975) of the inverse autocorrelation  $\Sigma_x \stackrel{def}{=} \mathbb{E}[\mathbf{x}\mathbf{x}^T]$  and the weight autocorrelation  $\Sigma_w \stackrel{def}{=} \mathbf{W}^T\mathbf{W}$ :

$$\hat{M} \stackrel{def}{=} \arg \max_M A(\mathbf{M}\mathbf{x}, \mathbf{W}\mathbf{M}^{-1}) = (\Sigma_w \# \Sigma_x^{-1})^{1/2}$$

$$\text{with } \mathbf{A} \# \mathbf{B} \stackrel{def}{=} \mathbf{A}^{1/2} \left( \mathbf{A}^{-1/2} \mathbf{B} \mathbf{A}^{-1/2} \right)^{1/2} \mathbf{A}^{1/2}. \quad (7)$$

Intuitively,  $\hat{M}$  maps the direction of variations of activations and weights into the same space:

$$\hat{M}\Sigma_x\hat{M} = \hat{M}^{-1}\Sigma_w\hat{M}^{-1} = \left( \Sigma_x^{-1/2}\Sigma_w\Sigma_x^{-1/2} \right)^{1/2}. \quad (8)$$

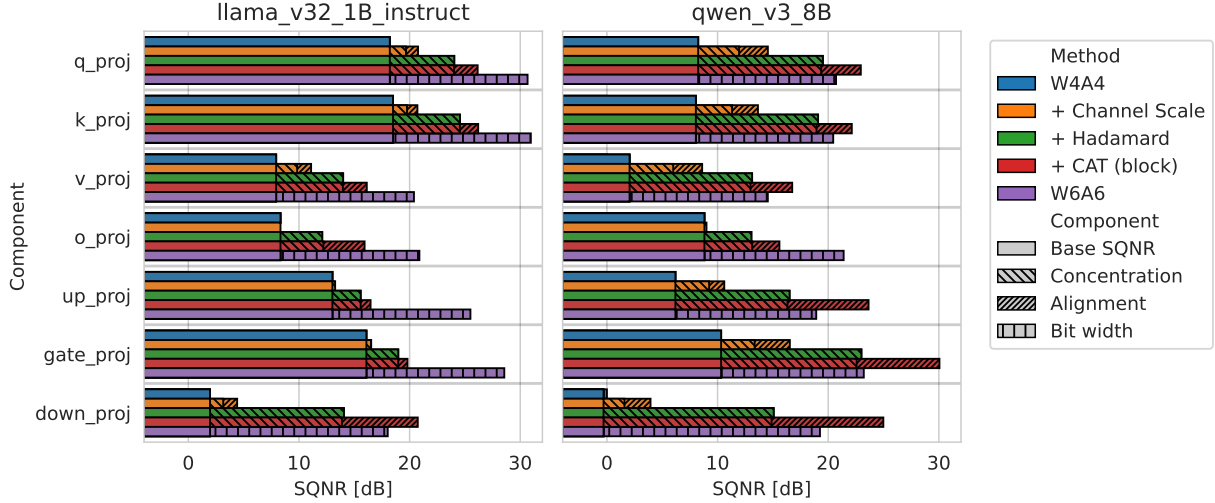


Figure 6. By designs transform for both alignment and concentration (CAT) drastically improve SQNR on all layers. In particular, Transformed W4A4 surpasses even W6A6 SQNR for all layers (except o\_proj) on the Qwen v3 8B architecture. Improvements are most notable for the MLP layers (gate, up, down), which have poor concentration and alignment without transforms.

The maximum value of alignment is determined by distribution of the eigenvalues of the layer output:

$$\begin{aligned}
 A(\hat{\mathbf{M}}\mathbf{x}, \mathbf{W}\hat{\mathbf{M}}^{-1}) &= \frac{\text{Tr}\left(\boldsymbol{\Sigma}_x^{-1/2}\boldsymbol{\Sigma}_w\boldsymbol{\Sigma}_x^{-1/2}\right)}{\text{Tr}\left(\left(\boldsymbol{\Sigma}_x^{-1/2}\boldsymbol{\Sigma}_w\boldsymbol{\Sigma}_x^{-1/2}\right)^{1/2}\right)^2} \\
 &= \frac{\sum_{i=1}^d \lambda_i^2}{\left(\sum_{i=1}^d \lambda_i\right)^2}, \quad (9)
 \end{aligned}$$

in which  $\lambda_i$  refer to the eigenvalues of  $\boldsymbol{\Sigma}_y \stackrel{def}{=} \mathbf{W}\boldsymbol{\Sigma}_x\mathbf{W}^T$ .

As demonstrated in Figure 5, alignment between model weights and activation is usually quite poor when compared to the best achievable value, indicated with a vertical green line. In particular, in large layers such as *down\_proj*, the alignment can be improved by about 10 dB, which would be roughly equivalent to the effect of increasing weight and activation by 2 bits each.

**Approximately optimal transform** Using the insights gained from the observations on alignment and concentration, we can design an approximately optimal transform  $\hat{\mathbf{T}}$  following a 2-step procedure:

1. We compute the invertible transformation  $\hat{\mathbf{M}}$  that maximizes alignment (equation 7).
2. We compose  $\hat{\mathbf{M}}$  with a Hadamard matrix  $\mathbf{H}$  that maximizes the (joint) concentration. Note that this operation does not affect the alignment since alignment is rotation-invariant.

Note that, in general,  $\hat{\mathbf{M}}$  is a full rank matrix, which is impractical for aligning weights and activations as it would require an expensive online matrix multiplication. In practice,  $\hat{\mathbf{M}}$  thus needs to be approximated by transforms that are cheaper, but which are not fully optimal for alignment. This yields numerous choices, e.g. diagonal (Xiao et al., 2024), Kronecker decompositions (Sun et al., 2025), or block-diagonal matrices, possibly with permutations of channels (Lin et al., 2024).

**CAT Block Approximation** We provide a simple block-diagonal example as a case study, which we refer to as Concentration Alignment Transform *CAT (block)* in this Section, and use this for the results in Section 6.

Let us consider a simple block-diagonal approximation  $\hat{\mathbf{M}}_{\text{block}}^k = \text{Diag}\left(\left[\hat{\mathbf{M}}_1, \dots, \hat{\mathbf{M}}_{d/k}\right]\right)$  composed of  $d/k$  blocks of size  $k$ , each optimized to maximize alignment on a subset of dimensions. This results in an approximately-optimal transform:

$$\hat{\mathbf{T}}_{\text{block}}^k \stackrel{def}{=} \mathbf{H}\hat{\mathbf{M}}_{\text{block}}^k. \quad (10)$$

Figure 4 and 5 report the values of concentration and alignment for  $\hat{\mathbf{T}}_{\text{block}}^k$  for  $k = 128$ . In all cases, we observe that  $\hat{\mathbf{T}}_{\text{block}}^k$  yields better concentration and alignment values resulting in higher SQNR. Figure 6 demonstrates that this simple transformation yields significant alignment improvement when compared to simple Hadamard rotations while retaining similar concentration levels. This results in gains of up to 10 dB in layers such as *gate\_proj* and *down\_proj*, exceeding the SQNR measured on a models quantized at 6 bits precision (in purple) on the Qwen v3 architecture.

Note that for  $k = 1$ , the expression for  $\hat{M}_{\text{block}}^k$  simplifies to a diagonal matrix  $\hat{M}_{\text{block}}^1 = \text{Diag}(\mathbf{m})$  in which each component is determined by the ratio between the expected squared weights and activations  $m_i = \sqrt{\mathbb{E}[x_i^2] / \sum_j w_{ij}^2}$ .

## 5. Related Work

Linear transformations are function-preserving operations (van Breugel et al., 2025) applied to the weights or activations of pretrained networks, such that the output of the network remains the same, yet the representation of the weights or distribution of the activations are more amenable to a downstream task. In particular, linear transformations are a popular for reducing outliers in LLMs and LVMs, and thereby improve quantization.

Xiao et al. (2024) note that activation quantization is more challenging than weight quantization because activations contain more outliers. They introduce SmoothQuant, which shifts these problematic activation outliers into the weights by applying a per-channel scaling factor to the activations entering linear layers. Chee et al. (2024) investigate transforms that mix channels, though only in the context of weight quantization. QuaRot (Ashkboos et al., 2024) popularized randomized Hadamard transforms (RHTs), demonstrating these effectively suppress outliers by spreading outlier channels across all other channels equally. SpinQuant (Liu et al., 2024) shows that different RHTs (i.e. different seeds) yield widely varying performance, yet the random component of RHTs is discrete and cumbersome to optimize. To address this, they extend QuaRot by introducing two unconstrained rotation matrices trained to minimize the standard causal language-modeling loss.

Importantly, these rotations are inserted so that they can be fused into the model weights after training, eliminating most runtime overhead. Lin et al. (2024) propose on-line rotations composed of fixed channel permutations and block-diagonal rotations. Note that by constraining FPTs to rotations, QuaRot, SpinQuant, and DuQuant can improve concentration, but not alignment. Newer works go beyond rotations. OSTQuant (Hu et al., 2025) integrates both scaling vectors and rotations.

Most recently, FlatQuant (Sun et al., 2025) introduces FPTs based on matrix multiplications with a Kronecker product of two smaller, invertible matrices, and train these to minimize quantization error. Although these non-rotation methods are motivated by outlier reduction, their training loss (per-block/end-to-end quantization error) can inadvertently also improve alignment. Concurrent work (Chen et al., 2026) derives an expression for optimal linear transformations by focusing on low-precision Floating Point quantization.

## 6. Experiments

**Models.** We choose a range of models to evaluate all methods. We use Llama 2 7B (Touvron et al., 2023), Llama 3 8B (Grattafiori et al., 2024) to allow direct comparison to reported results from QuaRot, SpinQuant, and FlatQuant. We add to this Llama 3.2 1B instruct as a small model that is popular for edge devices. We also include Ministral 8B instruct (Mistral.ai, 2025) and Qwen 3 8B to cover other model families.

**Calibration.** For all methods, we use 128 sequences of length 2048 of DCLM-edu for range setting and transform calibration/training. This is the same number as used in QuaRot and FlatQuant, though these related works calibrate on Wikitext. We prefer DCLM-edu, to ensure our Wikitext perplexity evaluation is not biased in favour of methods that may overfit the calibration data’s characteristics (observed in some related works, e.g. (van Breugel et al., 2025)).

**Quantization set-up.** We use the same set-up as used in QuaRot and follow-up works: linear layer inputs and weights in the transformer blocks and all KV cache is quantized. Activations and KV cache are quantized dynamically per token, asymmetrically, and weights are quantized per channel, symmetrically. For weight quantization, we run both round-to-nearest (RTN) and GPTQ (default settings) set-ups. We use  $L_{2.4}$  for weight range estimation, following GPTQ.

**Evaluation.** We evaluate Wikitext-2 perplexity at sequence length 2048 (Merity et al., 2017), and use LM-harness to evaluate the same common sense reasoning tasks used in FlatQuant (Sun et al., 2025): PIQA (Bisk et al., 2020), WinoGrande (Sakaguchi et al., 2021), Hel-laSwag (Zellers et al., 2019), ARC-e and ARC-c (Clark et al., 2018), and LAMBADA (Paperno et al., 2016).

**Baselines.** We compare block CAT (Section 4) with and without training, against the original floating point model (FP), PTQ using rounding-to-nearest (RTN), GPTQ (Frantar et al., 2022), prior rotation-based transforms QuaRot (Ashkboos et al., 2024) and SpinQuant (Liu et al., 2024), and the more expensive but state-of-the-art FlatQuant (Sun et al., 2025). To avoid differences in data, calibration, quantization, and evaluation set-up, we use the same pipeline for all methods.

**Results.** As reported in Table 1, in the RTN setting, we observe that without training *CAT (block)* outperforms all baselines on perplexity. On 0-shot performance, it performs comparable to the trained FlatQuant. With additional training, *CAT (block)* improves further—especially on 0-shot performance, where it generally outperforms FlatQuant.

Table 1. A CAT block diagonal matrix outperforms baselines, and performs on par even without training. Comparison of WikiText perplexity and averaged accuracy on six zero-shot common sense reasoning tasks. Average and standard deviation over 4 seeds.

Weight quantization	Transform method	Train	Llama 2 7B		Llama 3 8B		Llama 3.2 1B it		Ministral 8B it		Qwen 3 8B	
			Wiki (↓)	0-Shot <sup>6</sup> Avg.(↑)	Wiki (↓)	0-Shot <sup>6</sup> Avg.(↑)	Wiki (↓)	0-Shot <sup>6</sup> Avg.(↑)	Wiki (↓)	0-Shot <sup>6</sup> Avg.(↑)	Wiki (↓)	0-Shot Avg.(↑)
FP			5.47	69.46	6.14	73.43	13.16	59.95	6.97	74.36	9.73	70.18
RTN	None	✗	1621.86±0.00	31.51±0.00	321.22±0.00	35.31±0.00	412.51±0.00	32.18±0.00	63.59±0.00	38.81±0.00	23254.67±0.00	29.79±0.00
	SmoothQuant	✗	322.44±38.39	34.49±0.89	233.61±6.24	35.19±0.35	304.22±11.86	32.87±0.22	51.35±1.38	41.58±0.68	5047.04±1171.81	30.22±0.29
	QuaRot	✗	9.31±0.00	57.54±0.00	10.99±0.00	60.55±0.00	29.89±0.00	47.35±0.00	9.12±0.00	68.10±0.00	13.69±0.00	59.82±0.00
	CAT (block)	✗	<b>6.11±0.02</b>	<b>66.22±0.58</b>	<b>8.29±0.78</b>	<b>67.77±0.33</b>	<b>18.25±0.21</b>	<b>52.89±0.21</b>	<b>8.07±0.04</b>	<b>71.20±0.35</b>	<b>10.82±0.08</b>	<b>66.64±0.32</b>
	SpinQuant	✓	6.96±0.03	63.64±0.15	8.87±0.08	66.33±0.59	20.16±0.06	51.45±0.27	8.72±0.04	70.30±0.58	10.14±0.03	65.26±0.55
	FlatQuant	✓	6.05±0.01	66.67±0.17	7.61±0.01	68.34±0.09	17.63±0.22	54.14±0.24	7.95±0.03	71.86±0.32	10.69±0.04	66.25±0.37
GPTQ	CAT (block)	✓	<b>5.95±0.01</b>	<b>67.34±0.35</b>	<b>7.33±0.01</b>	<b>69.66±0.25</b>	<b>16.66±0.20</b>	<b>54.74±0.51</b>	<b>7.88±0.08</b>	<b>71.99±0.17</b>	<b>10.50±0.02</b>	<b>66.93±0.41</b>
	None	✗	1838.11±145.28	31.88±0.39	149.03±10.56	36.77±0.35	1514.48±202.46	32.66±0.54	30.62±0.17	45.93±0.62	19214.68±857.18	29.93±0.35
	SmoothQuant	✗	40.06±2.30	44.62±1.66	109.26±2.90	39.11±1.53	760.78±178.60	32.89±0.63	24.02±0.22	50.68±0.45	3306.28±340.65	30.00±0.25
	QuaRot	✗	6.22±0.02	66.06±0.27	8.21±0.02	67.15±0.19	19.97±0.19	50.93±0.30	8.18±0.03	71.19±0.47	11.50±0.07	64.61±0.53
	CAT (block)	✗	<b>6.01±0.02</b>	<b>67.25±0.14</b>	<b>7.60±0.04</b>	<b>68.32±0.49</b>	<b>17.89±0.15</b>	<b>54.15±0.53</b>	<b>7.94±0.02</b>	<b>71.74±0.11</b>	<b>10.58±0.14</b>	<b>67.14±0.68</b>
	SpinQuant	✓	6.26±0.03	66.12±0.38	7.88±0.05	68.75±0.41	18.16±0.11	53.80±0.16	8.28±0.01	71.39±0.15	9.94±0.06	65.59±0.42
GPTQ	FlatQuant	✓	<b>5.94±0.00</b>	<b>67.58±0.26</b>	<b>7.25±0.02</b>	<b>69.97±0.23</b>	<b>16.34±0.23</b>	<b>55.35±0.36</b>	<b>7.72±0.02</b>	<b>72.31±0.36</b>	<b>10.39±0.04</b>	<b>67.88±0.19</b>
	CAT (block)	✓	5.97±0.02	67.17±0.09	<b>7.25±0.01</b>	<b>70.38±0.43</b>	<b>16.33±0.07</b>	<b>55.39±0.17</b>	7.80±0.05	<b>72.26±0.16</b>	10.44±0.04	<b>67.83±0.42</b>

The GPTQ setting shows similar results, though now, baselines QuaRot and SmoothQuant have improved significantly compared to RTN, whereas GPTQ does not help *CAT (block)* w/ *train* or FlatQuant substantially, consistently with the results reported in (Sun et al., 2025). This is likely due to FlatQuant and CAT using learnable weight clipping during calibration, countering some of GPTQ’s benefits.

Comparing our baselines to Llama 2 7B and Llama 3 8B results reported in (Sun et al., 2025), our QuaRot is surprisingly better—likely due to switching to  $L_{2,4}$  range setting, in line with other methods. SpinQuant GPTQ achieves similar results: our perplexity numbers are as expected slightly worse due to switching from Wikitext to DCLM-edu for calibration, but 0-shot results are comparable. Similarly, the reported results are comparable to the ones reported in FlatQuant although the method has been re-implemented from scratch.

## 7. Conclusion

Low bit width quantization results in substantial errors, yet the community’s understanding of this error is limited. Recently, linear transforms prior to quantization (e.g. Hadamard transform) have become popular approaches to reducing errors, motivated by the idea of mixing large outliers into other channels. By decomposing linear layer quantization error into *Concentration* (a measure of outliers) and *Alignment* (a measure of the alignment of the data and weight principal directions), we show that outliers form only half of the quantization error story. We propose CAT, which designs transforms that improve both concentration and alignment.

**Limitations.** CAT provides the optimal transform for maximum alignment, but we note that this transform is a full-rank matrix that is costly and counterproductive for efficiency. This research does not prove what transforms may provide

the best speed-accuracy trade-off in approximating the CAT optimal transform. Nonetheless, in our results we show that a simple block-diagonal transform (similar in cost to FlatQuant) that approximates CAT, yields W4A4 results that are competitive even without training. Future research will explore better approximations —e.g. by adding mergeable rotations or permutations that can improve the block-diagonal approximation. Nonetheless, we believe that the proposed CAT framework provides actionable insights into effective design of linear transformations for effective low-precision quantization.

## Impact Statement

This paper’s goal is to improve the understanding of quantization error, and provide tools for creating more efficient AI models. This reduces the environmental footprint, latency, and economical cost of AI, and may improve access to AI in resource-constraint environments. However, it is important to recognize that quantization may affect biases of LLMs.

## References

Akhondzadeh, M. S., Bojchevski, A., Eleftheriou, E., and Dazzi, M. Kurtail : Kurtosis-based LLM quantization. *CoRR*, abs/2503.01483, 2025. doi: 10.48550/ARXIV.2503.01483. URL <https://doi.org/10.48550/arXiv.2503.01483>.

Ashkboos, S., Mohtashami, A., Croci, M. L., Li, B., Jaggi, M., Alistarh, D., Hoefler, T., and Hensman, J. QuaRot: Outlier-Free 4-Bit Inference in Rotated LLMs, March 2024. URL <https://arxiv.org/abs/2404.00456v1>.

Bisk, Y., Zellers, R., Bras, R. L., Gao, J., and Choi, Y. PIQA: Reasoning about Physical Commonsense in Natural Language. *Proceedings of the AAAI Confer-*

- ence on *Artificial Intelligence*, 34(05):7432–7439, April 2020. ISSN 2374-3468. doi: 10.1609/aaai.v34i05.6239. URL <https://ojs.aaai.org/index.php/AAAI/article/view/6239>. Number: 05.
- Chee, J., Cai, Y., Kuleshov, V., and De Sa, C. M. Quip: 2-bit quantization of large language models with guarantees. *Advances in Neural Information Processing Systems*, 36, 2024.
- Chen, J., Egiazarian, V., Castro, R. L., Hoefler, T., and Alistarh, D. Wush: Near-optimal adaptive transforms for llm quantization, 2026. URL <https://arxiv.org/abs/2512.00956>.
- Clark, P., Cowhey, I., Etzioni, O., Khot, T., Sabharwal, A., Schoenick, C., and Tafjord, O. Think you have Solved Question Answering? Try ARC, the AI2 Reasoning Challenge, March 2018. URL <http://arxiv.org/abs/1803.05457>. arXiv:1803.05457 [cs].
- Frantar, E., Ashkboos, S., Hoefler, T., and Alistarh, D. Gptq: Accurate post-training quantization for generative pre-trained transformers. *arXiv preprint arXiv:2210.17323*, 2022.
- Gersho, A. Quantization. *IEEE Communications Society Magazine*, 15:16–16, 1977. URL <https://api.semanticscholar.org/CorpusID:260498692>.
- Grattafiori, A., Dubey, A., Jauhri, A., Pandey, A., Kadian, A., Al-Dahle, A., Letman, A., Mathur, A., Schelten, A., Vaughan, A., et al. The llama 3 herd of models. *arXiv preprint arXiv:2407.21783*, 2024.
- Hu, X., Cheng, Y., Yang, D., Chen, Z., Xu, Z., JiangyongYu, XUCHEN, Yuan, Z., jiang, Z., and Zhou, S. OSTQuant: Refining Large Language Model Quantization with Orthogonal and Scaling Transformations for Better Distribution Fitting. In *The Thirteenth International Conference on Learning Representations*, 2025. URL <https://openreview.net/forum?id=rAcgDBdKnP>.
- Lin, H., Xu, H., Wu, Y., Cui, J., Zhang, Y., Mou, L., Song, L., Sun, Z., and Wei, Y. DuQuant: Distributing Outliers via Dual Transformation Makes Stronger Quantized LLMs. In *Advances in Neural Information Processing Systems*. arXiv, November 2024. doi: 10.48550/arXiv.2406.01721. URL <http://arxiv.org/abs/2406.01721>. arXiv:2406.01721.
- Liu, Z., Zhao, C., Fedorov, I., Soran, B., Choudhary, D., Krishnamoorthi, R., Chandra, V., Tian, Y., and Blankevoort, T. SpinQuant: LLM quantization with learned rotations, May 2024. URL <https://arxiv.org/abs/2405.16406v2>.
- Merity, S., Xiong, C., Bradbury, J., and Socher, R. Pointer sentinel mixture models. In *International Conference on Learning Representations*, 2017.
- Mistral.ai. Un minstral, des ministraux, 2025. URL <https://mistral.ai/news/ministraux>.
- Paperno, D., Kruszewski, G., Lazaridou, A., Pham, N.-Q., Bernardi, R., Pezzelle, S., Baroni, M., Boleda, G., and Fernández, R. The lambda dataset: Word prediction requiring a broad discourse context. In *Proceedings of the 54th Annual Meeting of the Association for Computational Linguistics (Volume 1: Long Papers)*, pp. 1525–1534, 2016.
- Pusz, W. and Woronowicz, S. Functional calculus for sesquilinear forms and the purification map. *Reports on Mathematical Physics*, 8(2):159–170, 1975. ISSN 0034-4877. doi: [https://doi.org/10.1016/0034-4877\(75\)90061-0](https://doi.org/10.1016/0034-4877(75)90061-0). URL <https://www.sciencedirect.com/science/article/pii/0034487775900610>.
- Sakaguchi, K., Bras, R. L., Bhagavatula, C., and Choi, Y. WinoGrande: an adversarial winograd schema challenge at scale. *Commun. ACM*, 64(9):99–106, August 2021. ISSN 0001-0782. doi: 10.1145/3474381. URL <https://dl.acm.org/doi/10.1145/3474381>.
- Shao, W., Chen, M., Zhang, Z., Xu, P., Zhao, L., Li, Z., Zhang, K., Gao, P., Qiao, Y., and Luo, P. OmniQuant: Omnidirectionally Calibrated Quantization for Large Language Models, March 2024. URL <http://arxiv.org/abs/2308.13137>. arXiv:2308.13137 [cs].
- Sun, M., Chen, X., Kolter, J. Z., and Liu, Z. Massive activations in large language models. *arXiv preprint arXiv:2402.17762*, 2024.
- Sun, Y., Liu, R., Bai, H., Bao, H., Zhao, K., Li, Y., JiaxinHu, Yu, X., Hou, L., Yuan, C., Jiang, X., Liu, W., and Yao, J. Flatquant: Flatness matters for LLM quantization. In *Forty-second International Conference on Machine Learning*, 2025. URL <https://openreview.net/forum?id=uTz2Uty5n>.
- Touvron, H., Martin, L., Stone, K., Albert, P., Almahairi, A., Babaei, Y., Bashlykov, N., Batra, S., Bhargava, P., Bhosale, S., et al. Llama 2: Open foundation and fine-tuned chat models. *arXiv preprint arXiv:2307.09288*, 2023.
- Tseng, A., Chee, J., Sun, Q., Kuleshov, V., and De Sa, C. QuIP#: Even Better LLM Quantization with Hadamard Incoherence and Lattice Codebooks, February 2024. URL <https://arxiv.org/abs/2402.04396v2>.

van Breugel, B., Bondarenko, Y., Whatmough, P., and Nagel, M. Fptquant: Function-preserving transforms for llm quantization. *arXiv preprint arXiv:2506.04985*, 2025.

Widrow, B., Kollar, I., and Liu, M.-C. Statistical theory of quantization. *IEEE Transactions on Instrumentation and Measurement*, 45(2):353–361, 1996. doi: 10.1109/19.492748.

Xiao, G., Lin, J., Seznec, M., Wu, H., Demouth, J., and Han, S. SmoothQuant: Accurate and Efficient Post-Training Quantization for Large Language Models, March 2024. URL <http://arxiv.org/abs/2211.10438>. arXiv:2211.10438 [cs].

Zellers, R., Holtzman, A., Bisk, Y., Farhadi, A., and Choi, Y. HellaSwag: Can a Machine Really Finish Your Sentence?, May 2019. URL <http://arxiv.org/abs/1905.07830>. arXiv:1905.07830 [cs].

## A. Proofs

### A.1. SQNR of quantized weights and activations

In order to demonstrate the statement reported in Lemma 2.1, we expand the quantization error for quantized weights and activations:

$$\begin{aligned}
 \mathbb{E} \left[ \left\| \mathbf{W}\mathbf{x} - \widetilde{\mathbf{W}}\widetilde{\mathbf{x}} \right\|_2^2 \right] &= \mathbb{E} \left[ \left\| \mathbf{W}\mathbf{x} - (\mathbf{W} - \Delta\mathbf{W})(\mathbf{x} - \Delta\mathbf{x}) \right\|_2^2 \right] \\
 &= \mathbb{E} \left[ \left\| \mathbf{W}\Delta\mathbf{x} + \Delta\mathbf{W}\mathbf{x} - \Delta\mathbf{W}\Delta\mathbf{x} \right\|_2^2 \right] \\
 &= \mathbb{E} \left[ \left\| \mathbf{W}\Delta\mathbf{x} \right\|_2^2 + \left\| \Delta\mathbf{W}\mathbf{x} \right\|_2^2 + \left\| \Delta\mathbf{W}\Delta\mathbf{x} \right\|_2^2 \right] \\
 &\quad + 2\mathbb{E} \left[ \text{Tr}(\mathbf{W}\Delta\mathbf{x}\mathbf{x}^T\Delta\mathbf{W}^T) - \text{Tr}(\mathbf{W}\Delta\mathbf{x}\Delta\mathbf{x}^T\Delta\mathbf{W}^T) - \text{Tr}(\Delta\mathbf{W}\mathbf{x}\Delta\mathbf{x}^T\Delta\mathbf{W}^T) \right] \\
 &= \mathbb{E} \left[ \left\| \mathbf{W}\Delta\mathbf{x} \right\|_2^2 \right] + \mathbb{E} \left[ \left\| \Delta\mathbf{W}\mathbf{x} \right\|_2^2 \right] + \mathbb{E} \left[ \left\| \Delta\mathbf{W}\Delta\mathbf{x} \right\|_2^2 \right] \\
 &\quad + 2\text{Tr}(\Delta\mathbf{W}^T\mathbf{W}\mathbb{E}[\Delta\mathbf{x}\mathbf{x}^T]) - 2\text{Tr}(\Delta\mathbf{W}^T\mathbf{W}\mathbb{E}[\Delta\mathbf{x}\Delta\mathbf{x}^T]) - 2\text{Tr}(\Delta\mathbf{W}^T\Delta\mathbf{W}\mathbb{E}[\mathbf{x}\Delta\mathbf{x}^T]) \\
 &\approx \mathbb{E} \left[ \left\| \mathbf{W}\Delta\mathbf{x} \right\|_2^2 \right] + \mathbb{E} \left[ \left\| \Delta\mathbf{W}\mathbf{x} \right\|_2^2 \right] = \mathbb{E} \left[ \left\| \mathbf{W}\mathbf{x} - \mathbf{W}\widetilde{\mathbf{x}} \right\|_2^2 \right] + \mathbb{E} \left[ \left\| \mathbf{W}\mathbf{x} - \widetilde{\mathbf{W}}\mathbf{x} \right\|_2^2 \right],
 \end{aligned}$$

in which  $\Delta\mathbf{x} \stackrel{def}{=} \mathbf{x} - \widetilde{\mathbf{x}}$  and  $\Delta\mathbf{W} \stackrel{def}{=} \mathbf{W} - \widetilde{\mathbf{W}}$ . This approximation is based on the following assumptions:

- The activations  $\mathbf{x}$  and the quantization noise  $\Delta\mathbf{x}$  are uncorrelated (Widrow et al., 1996):

$$\mathbb{E}[\Delta\mathbf{x}\mathbf{x}^T] \approx \mathbf{0}$$

- Similarly, the product between the weights  $\mathbf{W}$  and their quantization error  $\Delta\mathbf{W}$  is small:

$$\Delta\mathbf{W}^T\mathbf{W} \approx \mathbf{0}$$

- The magnitude of the product between the quantization noises is negligible:

$$\mathbb{E} \left[ \left\| \Delta\mathbf{W}\Delta\mathbf{x} \right\|_2^2 \right] \approx 0$$

Hence:

$$\begin{aligned}
 \text{SQNR}(\widetilde{\mathbf{W}}\widetilde{\mathbf{x}}) &= \frac{\mathbb{E} \left[ \left\| \mathbf{W}\mathbf{x} \right\|_2^2 \right]}{\mathbb{E} \left[ \left\| \mathbf{W}\mathbf{x} - \widetilde{\mathbf{W}}\widetilde{\mathbf{x}} \right\|_2^2 \right]} \\
 &\approx \frac{\mathbb{E} \left[ \left\| \mathbf{W}\mathbf{x} \right\|_2^2 \right]}{\mathbb{E} \left[ \left\| \mathbf{W}\mathbf{x} - \mathbf{W}\widetilde{\mathbf{x}} \right\|_2^2 + \left\| \mathbf{W}\mathbf{x} - \widetilde{\mathbf{W}}\mathbf{x} \right\|_2^2 \right]} \\
 &= \left( \frac{\mathbb{E} \left[ \left\| \mathbf{W}\mathbf{x} - \mathbf{W}\widetilde{\mathbf{x}} \right\|_2^2 \right] + \mathbb{E} \left[ \left\| \mathbf{W}\mathbf{x} - \widetilde{\mathbf{W}}\mathbf{x} \right\|_2^2 \right]}{\mathbb{E} \left[ \left\| \mathbf{W}\mathbf{x} \right\|_2^2 \right]} \right)^{-1} \\
 &= \left( \text{SQNR}(\mathbf{W}\widetilde{\mathbf{x}})^{-1} + \text{SQNR}(\widetilde{\mathbf{W}}\mathbf{x})^{-1} \right)^{-1} \\
 &= \text{SQNR}(\mathbf{W}\widetilde{\mathbf{x}}) \parallel \text{SQNR}(\widetilde{\mathbf{W}}\mathbf{x})
 \end{aligned} \tag{11}$$

## A.2. From SQNR to Concentration and Alignment

### A.2.1. ACTIVATION QUANTIZATION SQNR

We can express the MSE for a linear weight with quantized activations as:

$$\begin{aligned}\mathbb{E} \left[ \|\mathbf{W}\mathbf{x} - \mathbf{W}\tilde{\mathbf{x}}\|_2^2 \right] &= \mathbb{E} \left[ \|\mathbf{W}\Delta\mathbf{x}\|_2^2 \right] \\ &= \mathbb{E} \left[ \text{Tr}(\mathbf{W}\Delta\mathbf{x}\Delta\mathbf{x}^T\mathbf{W}^T) \right] \\ &= \text{Tr}(\mathbf{W}^T\mathbf{W}\mathbb{E}[\Delta\mathbf{x}\Delta\mathbf{x}^T]).\end{aligned}$$

Consider the autocorrelation term  $\mathbb{E}[\Delta\mathbf{x}\Delta\mathbf{x}^T]$ . We make the following assumptions

- The quantization noise has zero expectation:

$$\mathbb{E}[\Delta\mathbf{x}] \approx \mathbf{0}.$$

- The quantization noise for each channel is de-correlated:

$$\forall i \neq j \quad \mathbb{E}[\Delta\mathbf{x}_i\Delta\mathbf{x}_j] \approx \mathbb{E}[\Delta\mathbf{x}_i]\mathbb{E}[\Delta\mathbf{x}_j].$$

- The clipping error is negligible. For a given quantization bit width  $b_x$ ,

$$\lim_{b_x \rightarrow \infty} \Delta\mathbf{x} \approx \mathbf{0}$$

- All quantization intervals have the same size  $s_x$ , and the quantization noise is uniformly distributed in each interval:

$$\forall i \quad \Delta\mathbf{x}_i \sim \text{U}(-s_x/2, s_x/2), \quad (12)$$

with  $s_x \stackrel{\text{def}}{=} \frac{r(\mathbf{x})}{2^{b_x}-1}$  as the size of each quantization interval and  $r(\mathbf{x})$  as the full size of the quantized interval.

Given these assumptions, following classical work (Gersho, 1977), we have:

$$\mathbb{E}[\Delta\mathbf{x}_i\Delta\mathbf{x}_j] \approx \begin{cases} \mathbb{E}[\Delta\mathbf{x}_i]\mathbb{E}[\Delta\mathbf{x}_j] \approx 0 & \forall i \neq j \\ \mathbb{E}\left[\int_{-s/2}^{s/2} \frac{\Delta\mathbf{x}_i^2 d\Delta\mathbf{x}_i}{s}\right] = \mathbb{E}\left[\frac{s^2}{12}\right] & \forall i = j \end{cases}.$$

Hence:

$$\mathbb{E}[\Delta\mathbf{x}\Delta\mathbf{x}^T] \approx \mathbf{I} \frac{\mathbb{E}[r(\mathbf{x})^2]}{12(2^{b_x}-1)^2}.$$

Plugging this result in the previous expression:

$$\begin{aligned}\mathbb{E} \left[ \|\mathbf{W}\mathbf{x} - \mathbf{W}\tilde{\mathbf{x}}\|_2^2 \right] &\approx \frac{\mathbb{E}[r(\mathbf{x})^2]}{12(2^{b_x}-1)^2} \text{Tr}(\mathbf{W}^T\mathbf{W}) \\ &= \frac{1}{12(2^{b_x}-1)^2} \frac{\mathbb{E}[r(\mathbf{x})^2]}{\mathbb{E}[\|\mathbf{x}\|_2^2]} \|\mathbf{W}\|_F^2 \mathbb{E}[\|\mathbf{x}\|_2^2].\end{aligned}$$

Lastly, using this expression into the SQNR for quantized activations, we get:

$$\text{SQNR}(\mathbf{W}\tilde{\mathbf{x}}) \approx 12(2^{b_x}-1)^2 \underbrace{\frac{\mathbb{E}[\|\mathbf{x}\|_2^2]}{\mathbb{E}[r(\mathbf{x})^2]}}_{C(\mathbf{x})} \underbrace{\frac{\mathbb{E}[\|\mathbf{W}\mathbf{x}\|_2^2]}{\|\mathbf{W}\|_F^2 \mathbb{E}[\|\mathbf{x}\|_2^2]}}_{A(\mathbf{W},\mathbf{x})}. \quad (13)$$

### A.2.2. WEIGHT QUANTIZATION SQNR

The derivation for the SQNR for weight quantization is analogous to the one described for activation quantization. Here we underline the crucial steps

$$\begin{aligned} \mathbb{E} \left[ \left\| \mathbf{W}\mathbf{x} - \widetilde{\mathbf{W}}\mathbf{x} \right\|_2^2 \right] &= \mathbb{E} \left[ \sum_i^d \left\| \Delta \mathbf{w}_i^T \mathbf{x} \right\|_2^2 \right] \\ &= \text{Tr} \left( \sum_{i=1}^d (\Delta \mathbf{w}_i \Delta \mathbf{w}_i^T) \mathbb{E} [\mathbf{x} \mathbf{x}^T] \right). \end{aligned}$$

Here, the assumptions on  $\Delta \mathbf{w}_i$  are analogous to the ones enumerated for  $\Delta \mathbf{x}$ . Intuitively, whenever  $\mathbf{W}$  has a large number of rows  $d$ , we can treat the summation  $\sum_{i=1}^d (\Delta \mathbf{w}_i \Delta \mathbf{w}_i^T)$  as a (discrete) expectation  $d \mathbb{E} [\Delta \mathbf{w} \Delta \mathbf{w}^T]$  with  $\Delta \mathbf{w} \sim \text{Discrete}(\{\mathbf{w}_i\}_{i=1}^d, 1/d)$ . Therefore:

$$\sum_i \Delta \mathbf{w}_i \Delta \mathbf{w}_i^T \approx \mathbf{I} \frac{\sum_{i=1}^d r(\mathbf{w}_i)^2}{12(2^{b_w} - 1)^2}.$$

Plugging this result back into the previous expression:

$$\begin{aligned} \mathbb{E} \left[ \left\| \mathbf{W}\mathbf{x} - \widetilde{\mathbf{W}}\mathbf{x} \right\|_2^2 \right] &= \frac{\sum_i r(\mathbf{w}_i)^2}{12(2^{b_w} - 1)^2} \text{Tr} (\mathbb{E} [\mathbf{x} \mathbf{x}^T]) \\ &= \frac{1}{12(2^{b_w} - 1)^2} \frac{\sum_{i=1}^d r(\mathbf{w}_i)^2}{\sum_{i=1}^d \|\mathbf{w}_i\|_2^2} \mathbb{E} [\|\mathbf{x}\|_2^2] \|\mathbf{W}\|_F^2, \end{aligned}$$

hence:

$$\text{SQNR}(\widetilde{\mathbf{W}}\mathbf{x}) \approx 12(2^{b_w} - 1)^2 \underbrace{\frac{\sum_{i=1}^d r(\mathbf{w}_i)^2}{\sum_{i=1}^d \|\mathbf{w}_i\|_2^2}}_{C(\mathbf{W})} \underbrace{\frac{\mathbb{E} [\|\mathbf{W}\mathbf{x}\|_2^2]}{\|\mathbf{W}\|_F^2 \mathbb{E} [\|\mathbf{x}\|_2^2]}}_{A(\mathbf{W}, \mathbf{x})}. \quad (14)$$

### A.3. Full SQNR expression

We can combine the results from Equations 11, 13, and 14 to get a final expression:

$$\begin{aligned} \text{SQNR}(\widetilde{\mathbf{W}}\tilde{\mathbf{x}}) &\approx \text{SQNR}(\mathbf{W}\tilde{\mathbf{x}}) \|\text{SQNR}(\widetilde{\mathbf{W}}\mathbf{x}) \\ &\approx 12((2^{b_x} - 1)^2 C(\mathbf{x}) \|\mathbf{x}\|_2^2) \|(2^{b_w} - 1)^2 C(\mathbf{W}) A(\mathbf{x}, \mathbf{W}) \end{aligned} \quad (15)$$